A Twisting Donor-Acceptor Molecule with an Intercrossed Excited State for Highly Efficient, Deep-Blue Electroluminescence

Weijun Li, Dandan Liu, Fangzhong Shen, Dongge Ma, Zhiming Wang, Tao Feng, Yuanxiang Xu, Bing Yang, and Yuguang Ma**

In an organic electroluminescent (EL) device, the recombination of injected holes and electrons produces what appears to be an ion-pair or charge-transfer (CT) exciton, and this CT exciton decays to produce one photon directly, or relaxes to a low-lying local exciton (LE). Thus the full utilization of both the energy of the CT exciton and the LE should be a pathway for obtaining high-efficiency EL. Here, a twisting donor-acceptor (D-A) triphenylamine-imidazol molecule, TPA-PPI, is reported: its synthesis, photophysics, and EL performance. Prepared by a manageable, one-pot cyclizing reaction, TPA-PPI exhibits deep-blue emission with high quantum yields (90%) both in solution and in the solid state. Fluorescent solvatochromic experiments for TPA-PPI solutions show a red-shift of 57 nm (3032 cm^{-1}) from low-polarity hexane (406 nm) to high-polarity acetonitrile (463 nm), accompanied by the gradual disappearance of the vibrational band in the spectra with increased solvent polarity. The photophysical investigation and DFT analysis suggest an intercrossed CT and LE excited state of the TPA-PPI, originating from its twisting D-A configuration. This is a rare instance that a CT-state material shows highly efficient deep-blue emission. EL characterization demonstrates that, as a deep-blue emitter with CIE coordinates of (0.15, 0.11), the performance of a TPA-PPI-based device is rather excellent, displaying a maximum current efficiency of >5.0 cd A^{-1}, and a maximum external quantum efficiency of >5.0%, corresponding to a maximum internal quantum efficiency of >25%. The effective utilization of the excitation energy arising from materials with intercrossed-excited-state (LE and CT) characters is thought to be beneficial for the improved efficiency of EL devices.

1. Introduction

Light emission from an organic molecule occurs when it relaxes to its ground state by emitting a photon of light after being excited to a higher quantum state, or excited state, by absorption of some type of energy. The kind of excited state of the molecule determines its light-emitting properties, with regard to efficiency and energy. Organic light-emitting diodes (OLEDs), as one of the important applications of these luminescent molecules, have been widely studied.[1–7] In an OLED, the recombination of injected holes and electrons produces what appears to be an ion-pair or charge-transfer (CT) exciton, and this CT exciton decays to produce one photon directly, or relaxes to a low-lying local exciton (LE). Thus the full utilization of both the energy of the CT exciton and the LE may provide a pathway for obtaining high-efficiency electroluminescence (EL). Among OLED materials, the excited state with the CT feature has been proved to be very helpful in realizing the high efficiency of devices. For example, the widely used red dye 4-(dicyanomethylene)-2-methyl-6-[4-(dimethylaminostyryl)-4*H*-pyran] (DCM) and its derivatives possess typical CT characteristics with a strong fluorescence solvatochromic effect.[3] Phosphorescent metal complexes such as tris[2-phenylpyridinato-C^2,*N*] iridium(III) ($Ir(ppy)_3$) and bis[2-(4,6-difluorophenyl)pyridinato-C^2,*N*](picolinato)iridium(III) (FIrPic), which exhibit the highest device efficiency, also have excited states of a CT nature, so-called metal-to-ligand charge transfer (MLCT).[4] Great difficulty has been met in expanding CT materials from current red and green to blue and deep blue, because the CT excited-state usually possesses a narrower band gap than the normal local excited-state (LE) in the cases of both fluorescence and phosphorescence.[8,9] Considering the intrinsic wide-bandgap nature of deep-blue emitters, it is a really great challenge to achieve highly efficient deep-blue emission,[5] and it should be of significance if a solution were a CT-state material.

Dr. W. J. Li, Dr. D. D. Liu, Dr. F. Z. Shen, Dr. Z. M. Wang, T. Feng, Dr. Y. X. Xu, Prof. B. Yang, Prof. Y. G. Ma
State Key Lab of Supramolecular Structure and Materials
Jilin University
2699 Qianjin Avenue
Changchun, 130012, P.R. China
E-mail: yangbing@jlu.edu.cn; ygma@jlu.edu.cn
Prof. D. G. Ma
State Key Laboratory of Polymer Physics and Chemistry
Changchun Institute of Applied Chemistry
Chinese Academy of Sciences
Changchun 130022, P.R. China

DOI: 10.1002/adfm.201200116

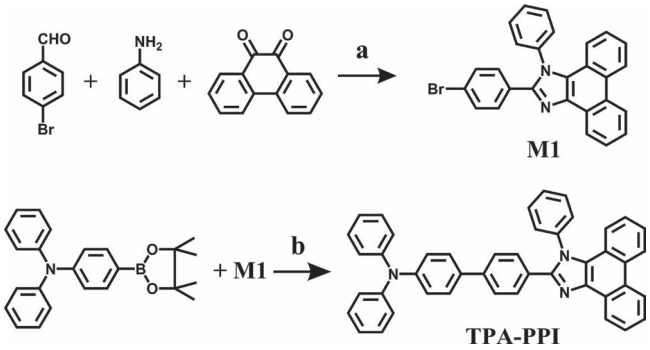

Scheme 1. The synthetic route to TPA-PPI (a: in CH_3COOH and ammonium acetate, refluxed for 2 h, yield: >80%; b: $Pd(PPh_3)_4$, sodium carbonate in toluene and distilled water, refluxed for 48 h under nitrogen, yield: 75%.)

Herein, we report our newly synthesized D-A molecule, TPA-PPI, based on a combination of triphenylamine (TPA) and 1,2-diphenyl-1H-phenanthro[9,10-d]imidazole (PPI). PPI is a highly efficient violet-blue chromophore with λ_{max} at 369 nm, developed by our group.[6] As PPI is modified by TPA to form a twisting, D-A molecule, TPA-PPI emits deep-blue light with $\lambda_{max} \approx 438$ nm, and an efficiency up to 90%, both in solution and as a film. Solvatochromic experiments indicate an intercrossed CT- and LE-state character for TPA-PPI in the excited state, which is thought to contribute to the observed very efficient fluorescence. By fabricating an EL device with TPA-PPI as the emitter, we got an excellent deep-blue EL performance with a maximum current efficiency of >5.0 cd A^{-1}, a maximum external quantum efficiency of >5.0%, and Commission Internationale de l'Eclairage (CIE) coordinates of (0.15, 0.11), which are among the best results reported.[7] As follows, we present our detailed experimental evidence and theoretical-calculation analysis.

2. Results and Discussion

2.1. Synthesis

The molecular structure and synthetic route of TPA-PPI are outlined in **Scheme 1**. TPA-PPI is composed of two main components: triphenylamine (TPA) as the donor moiety and 1,2-diphenyl-1H-phenanthro[9,10-d]imidazole (PPI) as the acceptor moiety. The preparation was accomplished by two main steps. Firstly, the important precursor, 2-(4-bromophenyl)-1-phenyl-1H-phenanthro[9,10-d]imidazole (M1), was synthesized by a one-pot cyclizing reaction via a mixture of aniline, phenanthrenequinone, ammonium acetate, and 4-bromobenzaldehyde, refluxed in acetic acid for 2 h. Then, through a Suzuki coupling reaction, we synthesized our terminal compound, TPA-PPI.

2.2. Excitation-State Properties

The UV and photoluminescence (PL) spectra of TPA-PPI in $CHCl_3$ solution are shown in **Figure 1**: the spectra of the compound PPI without the TPA substituent are also shown for comparison. Compared with the PPI, the absorption peak of TPA-PPI at around 365 nm becomes very strong, which can be ascribed to a newly generated CT transition from D (TPA) to A (PPI). This CT character of TPA-PPI was observed more obviously in the fluorescent measurements.

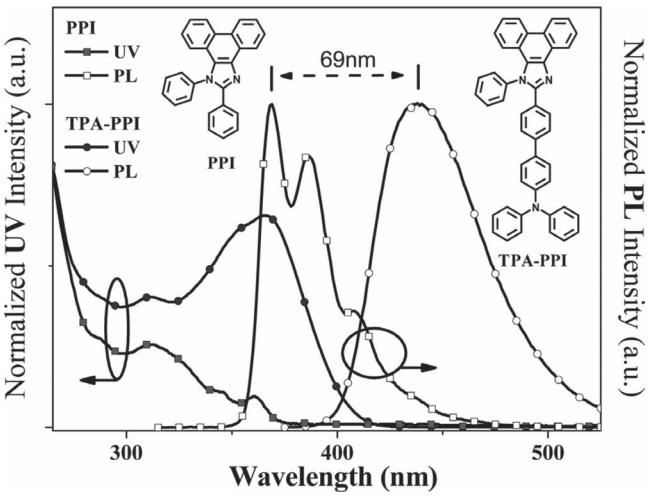

Figure 1. Normalized UV and PL spectra of TPA-PPI in $CHCl_3$ solution (10^{-5} M) with PPI for comparison.

Firstly, in contrast to PPI, which shows violet-blue emission at 369 nm with obvious vibronic structure features, TPA-PPI in the same solution of chloroform shows a large red-shift of 69 nm, with deep-blue emission at 438 nm and a broad PL spectrum without vibronic structure features. Secondly, as shown in **Figure 2**, in different polar solvents (such as hexane, ethyl acetate, and

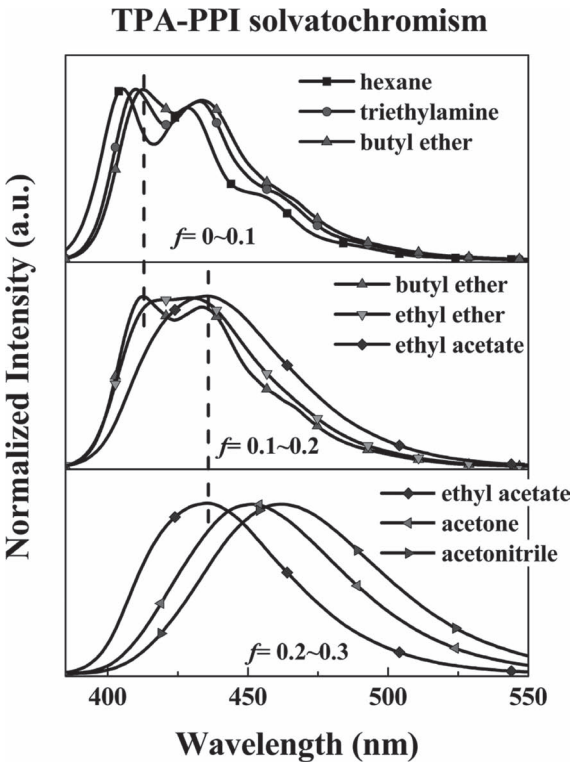

Figure 2. PL spectra of TPA-PPI, measured in different solvents with increasing polarity (the orientational polarizability of solvent, *f*, – hexane: 0.0012; triethylamine: 0.048; butyl ether: 0.096; ethyl ether: 0.167; ethyl acetate: 0.200; acetone: 0.284; and acetonitrile: 0.305 (Table S1, Supporting Information)).

acetonitrile), the solvatochromic effect of the PL spectra of TPA-PPI was observed. When the solvent polarity was increased gradually from low-polarity hexane to high-polarity acetonitrile, the TPA-PPI exhibited a large red-shift of 57 nm: 406 nm in hexane, 435 nm in ethyl acetate, and 463 nm in acetonitrile. This large solvatochromic shift, which is commonly consistent with the large dipole moment of the CT state, indicates that the low-lying excited state, S_1, of the TPA-PPI possesses a strong-CT-state characteristic.[8]

The dipole moment of the S_1 state can be estimated from the slope of a plot of the Stokes shift ($\nu_a - \nu_f$) against the solvent parameters, or the orientation polarizability $f(\varepsilon,n)$, according to the Lippert–Mataga[8] equation:

$$hc(\nu_a - \nu_f) = hc(\nu_a^0 - \nu_f^0) + \frac{2(\mu_e - \mu_g)^2}{a^3} f(\varepsilon, n)$$

where f is the orientational polarizability of the solvent, $\nu_a^0 - \nu_f^0$ corresponds to the Stokes shifts when f is zero, μ_e is the excited-state dipole moment, μ_g is the ground-state dipole moment, a is the solvent Onsager cavity radius, and ε and n are the solvent dielectric and the solvent refractive index, respectively (Table S1, Supporting Information) (see the solvatochromic-effect part in the supporting information).

Obviously, the experimental data do not obey the linear relationship predicted by the Lippert–Mataga equation well, in the whole range of solvent polarity, as shown in **Figure 3**. A transformation in the slope of the fitted line is observed between the butyl ether (f = 0.10) and ethyl acetate (f = 0.20) solvents. Through the analysis of the fitted line in high-polarity solvents, a slope value of ≈14 272 (R = 0.96) was obtained. The ground-state dipole, μ_g, of the TPA-PPI could be estimated from a long-range-correction density-functional-theory (DFT) calculation using the Gaussian 09 package[10a] (CAM-B3LYP/Coulomb-attenuating method-B3LYP[10b,c] at the basis set level of 6-31G*), which gave a μ_g of 4.09 D. Thus, the corresponding excited-state dipole, μ_e, was calculated to be 18.5 D for TPA-PPI in high-polarity solvents, according to the Lippert–Mataga equation. In the region of low-polarity solvents, a linear relationship with a slope of near zero could be drawn for TPA-PPI, indicating no obvious change between μ_e and μ_g. However, we could not obtain the exact value of μ_e, because the slope was so small that a tiny deviation from the linear line would cause prodigious R values. Thus, the small μ_e was estimated to be close to 4.09 D for TPA-PPI in low-polarity solvents. This small μ_e of 4.09 D can be attributed to the usual excited-state,[8,9] which is a LE state, while the large μ_e of 18.5 D should not be treated as a small parameter in contrast to the usual excited states (LE). It is actually smaller than, but very close to, the μ_e value of 4-(*N*,*N*-dimethylamino)-benzonitrile (DMABN), a typical CT molecule, which has $\mu_e \approx 23$ D.[8] The fluorescent solvatochromic experiments and non-linear relationship of the Stokes shift with solvent polarity indicate that our molecule, TPA-PPI, possesses the intercrossed excited state of LE and CT: a bigger contribution from the CT state in high-polarity solvents ($f \geq 0.2$), a bigger contribution from the LE state in low-polarity solvents ($f \leq 0.1$), and a totally intercrossed excited state of the LE and CT in moderately polar environments between butyl ether and ethyl acetate, or at the polarity level near chloroform.

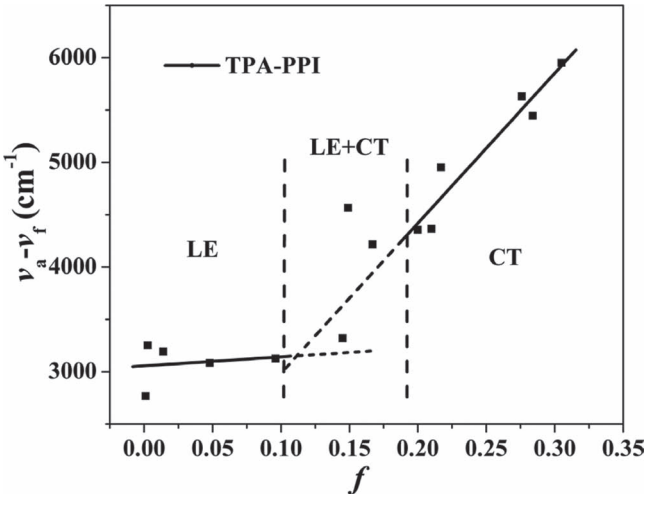

Figure 3. Linear correlation of orientation polarization (f) of solvent media with the Stokes shift ($\nu_a - \nu_f$) for TPA-PPI. (See Table S1 for data; the lines in the high- and low-polarity regions were fitted to the points with $f \geq 0.2$ and $f \leq 0.1$, respectively; the dashed parts of the fitted lines are the extrapolated parts of them.)

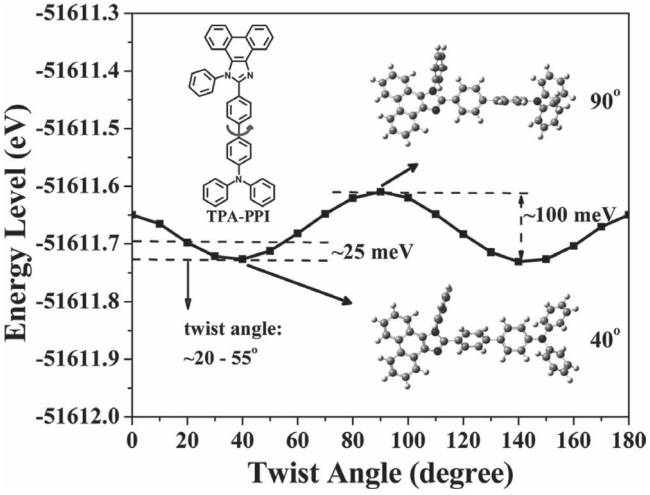

Figure 4. The ground-state energy of TPA-PPI at different biphenyl twist angles in the gas phase, using the cam-b3lyp method and a full geometrical optimization at each twist angle.

DFT analysis of the molecular configuration and frontier molecular orbital revealed that a twisting D-A linking with an angle of 20–55° should be the origin of the CT and LE intercross. The ground-state energy of TPA-PPI and the corresponding electronic density distribution of the frontier molecular orbitals (highest occupied molecular orbital (HOMO) and lowest unoccupied molecular orbital (LUMO)) at twist angles of 40° and 90° are shown in **Figure 4** and **Figure 5**, respectively. At a twist angle of 90°, we can see the obviously separated HOMO and LUMO on the TPA and PPI, respectively, which generates a pure-CT transition of HOMO (donor) → LUMO (acceptor) in the TPA-PPI. However, TPA-PPI in such a 90° twisting conformation is unstable, because its energy is ≈0.1 eV higher than that of TPA-PPI at a twist angle of ≈40°, based on DFT total-energy analysis. In TPA-PPI with a D-A twisting of ≈40°, which is the lowest-energy conformation, both the HOMO and the LUMO partially delocalize to the whole TPA-PPI molecule, instead of there being

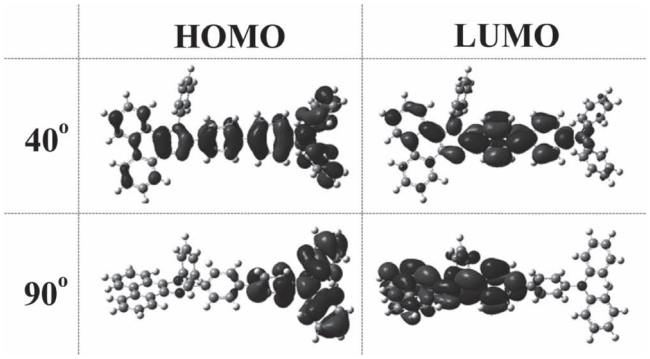

Figure 5. The frontier molecular orbitals (HOMO and LUMO) in the ground state of TPA-PPI at different biphenyl twist angles (the isovalue was set to be 0.02 a.u.).

a fully separated (or localized) HOMO and LUMO. In this case, HOMO → LUMO should not be treated as a pure-CT transition, but an intercrossed transition of CT and $\pi \rightarrow \pi^*$. Naturally, the intercrossed molecular orbitals bring the intercrossed character of the LE and CT states. When in different polar solvents, the LE and CT states show different properties because of their different excited-state dipole moments. As the solvent polarity increases, the CT energy level starts to decrease, due to strong interaction of the solvent field with the CT excited state (large dipole moment), while LE remains nearly unchanged.[8,9] In low-polarity solvents, the LE, being the low-lying excited state, dominates the luminescence with well-resolved LE emission features. With increased solvent polarity, a depressed CT energy, which is close to energy of the LE, results in both LE and CT emissions simultaneously, like an intercrossing of the LE and CT states. In solvents with very high polarity, the CT state may become the lowest excited state, resulting in broad and red-shifted CT emissions.

With TPA-PPI as a film and as a bulk solid (the main form for applications), its spectral character was very similar to that of TPA-PPI in chloroform (Figure S2 and **Table 1**). This indicates that the solid state (film) has a similar polar-environment effect on the TPA-PPI molecule to that of chloroform, in which TPA-PPI has been proved to possess the intercrossed excited state. Thus, TPA-PPI in a film should also retain the character of the intercrossed excited state. The measurement of the fluorescent quantum yield, by using quinine sulphate in 1 M sulphuric acid as a standard, demonstrated a value as high as 90% for TPA-PPI in chloroform, and the fluorescence quantum yield of TPA-PPI film, determined using an integrating-sphere photometer, was also 90%. This is a rare instance that a CT state material shows highly efficient deep-blue emission. It is highly possible that the reason for the exceptionally high fluorescence yield is the coexistence of the emissions from the LE and the CT (or, to put it another way, an intercrossed CT and LE state). As evidence, as shown in Table S3, the oscillator strengths for absorption and emission were both enlarged in the moderately polar solvent chloroform, in contrast to that in the gas phase, which indicates the higher luminescence of the intercrossed excited state in chloroform; further evidence is that the low-lying CT state that dominates the luminescence results in a greatly decreased efficiency in high-polarity environments, as shown in Table S1.

2.3. Electroluminescence Properties

TGA and DSC measurements have shown that TPA-PPI is a highly thermally stable material. Its glass-transition temperature (T_g) is 130 °C, and its thermal-decomposition temperature (T_d) at 5% weight loss is 475 °C (Figure S4). Atomic-force-microscopy (AFM) measurements showed that TPA-PPI film exhibits a fairly smooth surface morphology with a roughness of 0.79 nm, which was nearly unchanged after annealing at 90 °C for 2 h (Figure S5). These results indicate that TPA-PPI can form a very stable and smooth film to support EL device fabrication. Cyclic-voltammetry analysis was also carried out, which gave HOMO and LUMO levels of –5.18 eV and –2.27 eV, respectively, for TPA-PPI (Figure S3).

To investigate the EL properties of TPA-PPI, we constructed a device with a frequently used multilayered structure: indium tin oxide (ITO)/MoO_3 (10 nm)/N,N′-di-1-naphthyl-N,N′-diphenylbenzidine (NPB) (80 nm)/4,4′,4″-tri(N-carbazolyl)-triphenylamine (TCTA) (5 nm)/TPA-PPI (20 nm)/1,3,5-tri(phenyl-2-benzimidazolyl)-benzene (TPBi) (40 nm)/LiF (1 nm)/Al (100 nm), in which MoO_3 was utilized as a hole-injecting layer, NPB and TCTA as hole-transporting and buffer layers, and TPBi as an electron-transporting and hole-blocking layer. From the EL spectrum, shown in **Figure 6**b, we could see a obvious deep-blue emission with λ_{max} at 434 nm and little vibronic feature. Such an EL spectrum is very similar to PL spectra observed from chloroform solution and films, indicating the same source of EL and PL, most likely the intercrossed LE and CT excited-state of the TPA-PPI.

This device exhibited excellent performance with a maximum luminance of 13 675 cd m^{-2}, power efficiency > 6.0 lm W^{-1}, current efficiency > 5.0 cd A^{-1}, and maximum external quantum efficiency (η_{ext}) > 5.0%, as shown in Figure 6a, **Figure 7**a and **Table 2**. Through calculation from the relationship $\eta_{ext} = \eta_{int} \cdot \eta_{ph}$, assuming a light out-coupling efficiency of $\eta_{ph} \approx 1/(2n^2) \approx 20\%$ for a glass substrate with an index

Table 1. The thermal, photophysical, and electrochemistry data of TPA-PPI.

	T_g [°C]	T_d[a)] [°C]	UV (soln) [nm]	PL λ_{max} (soln) [nm]	UV (film) [nm]	PL λ_{max} (film) [nm]	Φ_{fl} (soln/film)[b)]	HOMO[c)] [eV]	LUMO[c)] [eV]
TPA-PPI	130	475	365	438	368	440	0.90/0.90	–5.22	–2.27

[a)]The temperature for 5% weight loss of the materials; [b)]The fluorescence quantum yield was measured in solution using a 0.5 M H_2SO_4 solution of quinine as a reference (0.54); the solid - state quantum yield on the quartz plate was measured using an integrating - sphere apparatus; [c)]Estimated based on cyclic - voltammetry (CV) data of each compound by comparing with ferrocene (Fc) (4.8 eV).

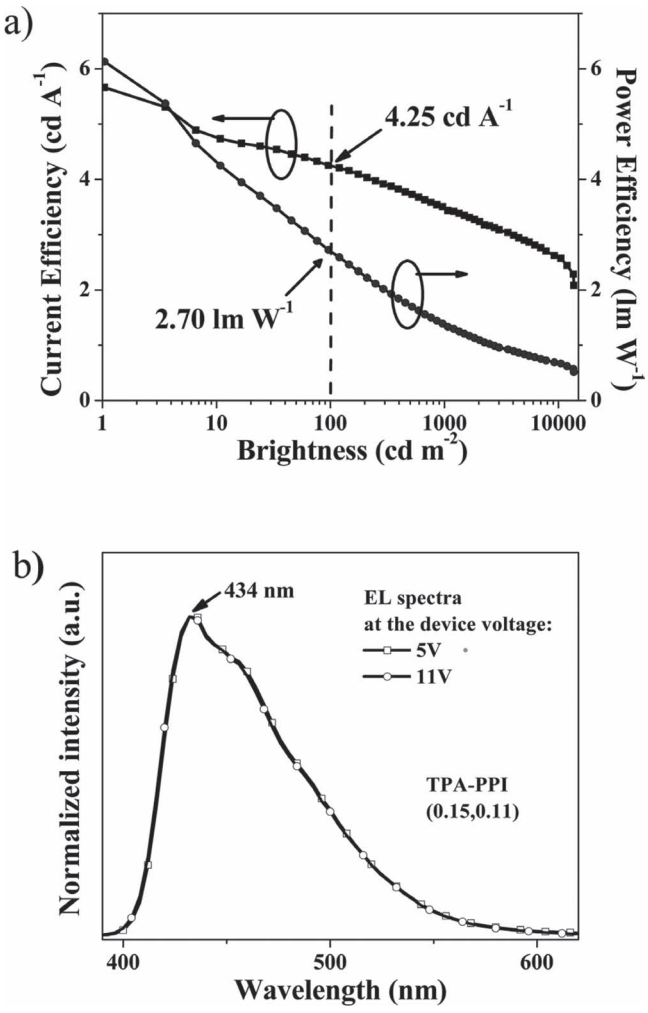

Figure 6. a,b) The current-efficiency–luminance–power-efficiency curves (a) and EL spectra at different operation voltages (b) of a device with TPA-PPI as the emitter.

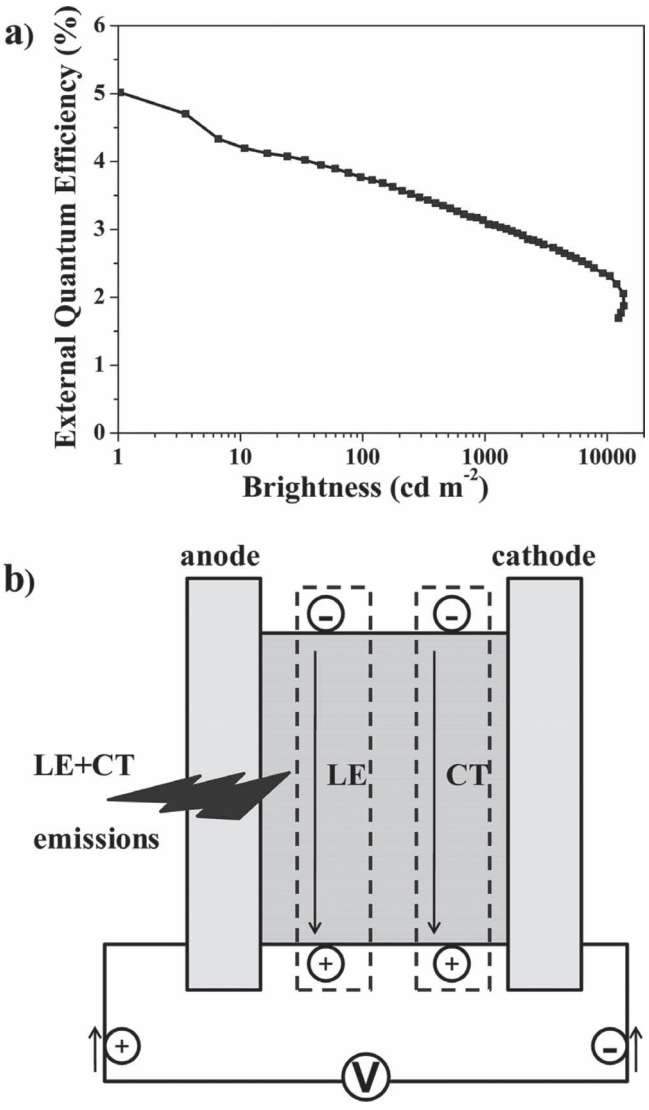

Figure 7. a) The external efficiency–luminance curve of a device with TPA-PPI as the emitter. b) The simple scheme of recombination of electrons and holes in our device with TPA-PPI as the emitter, which has the intercrossed LE and CT state.

of refraction $n = 1.5$, we tuned the η_{ext} to the corresponding maximum internal quantum efficiency $\eta_{int} > 25\%$. Considering the TPA-PPI fluorescent quantum efficiency < 100% (90%) and spin statistics (1/4), in the case of our EL device, actually, the limit of the η_{int} was smaller than 25%.[11] This indicates that TPA-PPI devices break through the limit of η_{int} ruled by spin statistics, which is just found in triplet phosphorescence materials and special singlet materials.[12] This breakthrough of η_{int} is tentatively proposed to be owing to the fully effective utilization of both the energy of the LE and the CT exciton, including singlets, ^{1}CT, and triplets, ^{3}CT, because it is possible for the transition $^3CT \rightarrow {}^1CT$ to become allowed due to the energetic closeness between ^{1}CT and ^{3}CT.[13] The main reason for the high device efficiency is having both the LE and CT emissions simultaneously in the device, arising from the intercrossed excited-state (LE and CT) in the TPA-PPI emitter.

Table 2. The device performance of TPA-PPI.

Device	CIE coordinates [x, y]	EQE_{max} [%]	LE_{max} [cd A^{-1}]	PE_{max} [lm W^{-1}]	L_{max} [cd m^{-2}]	Device performance at 100 cd m^{-2}		
						EQE [%]	LE [cd A^{-1}]	PE [lm W^{-1}]
TPA-PPI	0.15, 0.11	5.02	5.66	6.13	13 675	3.76	4.25	2.70

Moreover, based on luminances of 100 cd m^{-2} (or 1000 cd m^{-2}), the TPA-PPI device also showed a high current efficiency of 4.25 cd A^{-1} (or 3.50 cd A^{-1}) and an external quantum efficiency (EQE) of 3.76% (or 3.13%), which are among the best results of nondoped deep-blue OLED structures that have been reported.[7] The EL spectra showed the TPA-PPI device performed with quite excellent color stability in the whole voltage range at the same CIE coordinates of (0.15, 0.11), as shown in Figure 6b.

3. Conclusions

In summary, the intercrossed excited state has been demonstrated to exist in a twisting D-A molecule, TPA-PPI, through a combined photophysical and DFT investigation. This intercrossed excited state, with simultaneous LE and CT emission, is responsible for the observed high quantum efficiency both in solution and as a film. Such a special material is very suitable for OLED applications. A nondoped device with TPA-PPI as the emitter reached an internal quantum efficiency (η_{int}) of >25%, breaking through the limit of η_{int} for fluorescence-based EL devices. The effective utilization of the excitation energy arising from the intercrossed excited-state (LE and CT) is thought to contribute to the improved efficiency. In this article, new insight into the excited state of the twisting D-A molecules provides us with an effective strategy to construct highly efficient OLED materials that employ the intercrossed excited state of the LE and CT.

4. Experimental Section

All of the reagents and solvents used for the syntheses were purchased from Aldrich or Acros and were used as received. All of the reactions were performed under a dry-nitrogen atmosphere. The 1H NMR spectra were recorded on AVANCZ 500 spectrometers at 298 K by utilizing deuterated dimethyl sulfoxide (DMSO) as solvents and tetramethylsilane (TMS) as a standard. The compounds were characterized by a Flash EA 1112, CHNS-O elemental analysis instrument. The MALDI-TOF-MS mass spectra were recorded using an AXIMA-CFRTM plus instrument. UV-vis absorption spectra were recorded on a UV-3100 spectrophotometer. Fluorescence measurements were carried out with a RF-5301PC.

Synthesis of 2-(4-Bromophenyl)-1-phenyl-1H-phenanthro[9,10-d]-imidazole (M1): A mixture of aniline (10.0 mmol), phenanthrenequinone (2.0 mmol), 4-bromobenzaldehyde (2.0 mmol), ammonium acetate (8.0 mmol), and acetic acid (15 mL) was refluxed under nitrogen in an oil bath. After 2 h, the mixture was cooled and filtered. The solid product was washed with an acetic acid/water mixture (1:1, 30 mL) and water. Then, it was dried in the vacuum and used directly for the next step without further purification and characterization. ^{1}H NMR (500 MHz, DMSO, 25 °C, TMS, δ): 8.94 (d, J = 8.4 Hz, 1H, Ar H), 8.89 (d, J = 8.4 Hz, 1H, Ar H), 8.69 (d, J = 8.0 Hz, 1H, Ar H), 7.79 (t, J = 7.4 Hz, 1H, Ar H), 7.77–7.68 (m, 6H, Ar H), 7.58 (m, 3H, Ar H), 7.52 (d, J = 8.4 Hz, 2H, Ar H), 7.35 (t, J = 7.7 Hz, 1H, Ar H), 7.09 (d, J = 8.3 Hz, 1H, Ar H); MALDI-TOF MS (mass m/z): 449.0 [M^+ + H].

Synthesis of N,N-Diphenyl-4′-(1-phenyl-1H-phenanthro[9,10-d]imidazol-2-yl)biphenyl-4-amine (TPA-PPI): A mixture of *N*,*N*-diphenyl-4-(4,4,5,5-tetramethyl-1,3,2-dioxaborolan-2-yl)aniline (449.4 mg, 1.0 mmol) (synthesized by: n-butyl-lithium added into 4-bromo-*N*,*N*-diphenylaniline at –78 °C, then 2-isopropoxy-4,4,5,5-tetramethyl-1,3,2-dioxabrorolane added, and the mixture stirred for 24 h at room temperature), M1 (408.4 mg, 1.1 mmol), sodium carbonate (635.9 mg, 6.0 mmol), toluene (4.5 mL), and distilled water (3.0 mL), with tetrakis(triphenylphosphine) palladium(0) ($Pd(PPh_3)_4$) (50 mg) acting as catalyst, was refluxed at 90 °C for 48 h under nitrogen. Then, some water was added to the resulting solution and the mixture was extracted with chloroform several times. The organic phase was dried over anhydrous magnesium sulfate. After filtration and solvent evaporation, the liquid was purified by column chromatography using petroleum ether/CH_2Cl_2 as the eluent to afford a white solid. Yield: 75%; ^{1}H NMR (500 MHz, DMSO, 25 °C, TMS, δ): 8.94 (d, J = 8.2 Hz, 1H, Ar H), 8.89 (d, J = 8.2 Hz, 1H, Ar H), 8.72 (d, J = 7.8 Hz, 1H, Ar H), 7.83–7.68 (m, 7H, Ar H), 7.64 (d, J = 6.2 Hz, 6H, Ar H), 7.57 (t, J = 7.4 Hz, 1H, Ar H), 7.34 (t, J = 7.9 Hz, 5H, Ar H), 7.11–7.06 (m, 7H, Ar H), 7.03 (d, J = 8.6 Hz, 2H, Ar H); ^{13}C NMR (126 MHz, $CDCl_3$, 25 °C, TMS, δ): = 150.71 (C), 147.59 (C), 140.76 (C), 138.89 (C), 137.53 (C), 133.93 (C), 130.22 (CH), 129.83 (CH), 129.73 (CH), 129.33 (CH), 129.19 (CH), 128.87 (CH), 128.30 (C), 128.23 (C), 127.65 (CH), 127.23 (CH), 126.27 (CH), 126.24 (CH), 125.64 (CH), 124.88 (CH), 124.54 (CH), 124.14 (CH), 123.74 (CH), 123.12 (CH), 123.10 (CH), 122.84 (CH), 120.88 (CH); MALDI-TOF MS (mass m/z): 615.6 [M^+ + H]; Anal. calcd for $C_{45}H_{31}N_3$: C 88.06, H 5.09, N 6.85; found: C 88.46, H 5.35, N 6.37.

Supporting Information

Supporting Information is available from the Wiley Online Library or from the author.

Acknowledgements

We are grateful for support from the National Science Foundation of China (51073069, 20834006), the Ministry of Science and Technology of China (2009CB623605), and PCSIRT (20921003).

Received: January 13, 2012
Revised: February 9, 2012
Published online: April 16, 2012

[1] C. W. Tang, S. A. VanSlyke, *Appl. Phys. Lett.* **1987**, *51*, 93.
[2] Y. G. Ma, H. Zhang, J. C. Shen, C. Che, *Synth. Met.* **1998**, *94*, 245.
[3] a) C. H. Chen, C. W. Tang, J. Shi, K. P. Klunek, *Macromol. Symp.* **1997**, *125*, 49; b) C. Q. Ma, B. X. Zhang, Z. Liang, P. H. Xie, X. S. Wang, B. W. Zhang, Y. Cao, X. Y. Jiang, Z. L. Zhang, *J. Mater. Chem.* **2002**, *12*, 1671; c) Y. S. Yao, J. Xiao, X. S. Wang, Z. B. Deng, B. W. Zhang, *Adv. Funct. Mater.* **2006**, *16*, 709.
[4] a) S. J. Su, E. Gonmori, H. Sarabe, J. Kido, *Adv. Mater.* **2008**, *20*, 4189; b) F. M. Hsu, C. H. Chien, C. F. Shu, C. H. Lai, C. C. Hsieh, K. W. Wang, P. T. Chou, *Adv. Funct. Mater.* **2009**, *19*, 2834; c) Y. Tao, Q. Wang, C. L. Yang, C. Zhong, K. Zhang, J. G. Qin, D. G. Ma, *Adv. Funct. Mater.* **2010**, *20*, 304; d) S. O. Jeon, S. E. Jang, H. S. Son, J. Y. Lee, *Adv. Mater.* **2011**, *23*, 1436.
[5] a) B. Wei, J. Z. Liu, Y. Zhang, J. H. Zhang, H. N. Peng, H. L. Fan, Y. B. He, X. C. Gao, *Adv. Funct. Mater.* **2010**, *20*, 2448; b) Z. Q. Jiang, Z. Y. Liu, C. L. Yang, C. Zhong, J. G. Qin, G. Yu, Y. Q. Liu, *Adv. Funct. Mater.* **2009**, *19*, 3987; c) C. G. Zhen, Z. K. Chen, Q. D. Liu, Y. F. Dai, R. Y. C. Shin, S. Y. Chang, J. Kieffer, *Adv. Mater.* **2009**, *21*, 2425.
[6] Z. M. Wang, P. Lu, S. M. Chen, Z. Gao, F. Z. Shen, W. S. Zhang, Y. X. Xu, H. S. Kwok, Y. G. Ma, *J. Mater. Chem.* **2011**, *21*, 5451.
[7] a) P. I. Shih, C. Y. Chuang, C. H. Chien, E. W.-G. Diau, C. F. Shu, *Adv. Funct. Mater.* **2007**, *17*, 3141; b) L. Wang, Y. Jiang, J. Luo, Y. Zhou, J. H. Zhou, J. Wang, J. Pei, Y. Cao, *Adv. Mater.* **2009**, *21*, 4854; c) K. C. Wu, P. J. Ku, C. S. Lin, H. T. Shih, F. I. Wu, M. J. Huang, J. J. Lin, I. C. Chen, C. H. Cheng, *Adv. Funct. Mater.* **2008**, *18*, 67.
[8] Z. R. Grabowski, K. Rotkiewicz, W. Rettig, *Chem. Rev.* **2003**, *103*, 3899.

[9] a) S. M. King, I. I. Perepichka, I. F. Perepichka, F. B. Dias, M. R. Bryce, A. P. Monkman, *Adv. Funct. Mater.* **2009**, *19*, 586; b) J. Herbich, A. Kapturkiewicz, *J. Am. Chem. Soc.* **1998**, *120*, 1014.

[10] a) M. J. Frisch, G. W. Trucks, H. B. Schlegel, G. E. Scuseria, M. A. Robb, J. R. Cheeseman, G. Scalmani, V. Barone, B. Mennucci, G. A. Petersson, H. Nakatsuji, M. Caricato, X. Li, H. P. Hratchian, A. F. Izmaylov, J. Bloino, G. Zheng, J. L. Sonnenberg, M. Hada, M. Ehara, K. Toyota, R. Fukuda, J. Hasegawa, M. Ishida, T. Nakajima, Y. Honda, O. Kitao, H. Nakai, T. Vreven, J. A. Montgomery Jr., J. E. Peralta, F. Ogliaro, M. Bearpark, J. J. Heyd, E. Brothers, K. N. Kudin, V. N. Staroverov, R. Kobayashi, J. Normand, K. Raghavachari, A. Rendell, J. C. Burant, S. S. Iyengar, J. Tomasi, M. Cossi, N. Rega, J. M. Millam, M. Klene, J. E. Knox, J. B. Cross, V. Bakken, C. Adamo, J. Jaramillo, R. Gomperts, R. E. Stratmann, O. Yazyev, A. J. Austin, R. Cammi, C. Pomelli, J. W. Ochterski, R. L. Martin, K. Morokuma, V. G. Zakrzewski, G. A. Voth, P. Salvador, J. J. Dannenberg, S. Dapprich, A. D. Daniels, Ö. Farkas, J. B. Foresman, J. V. Ortiz, J. Cioslowski, D. J. Fox, Gaussian 09, revision A.02, Gaussian, Inc., Wallingford, CT, USA **2009**; b) T. Yanai, D. P. Tew, N. C. Handy, *Chem. Phys. Lett.* **2004**, *393*, 51; c) T. Yanai, R. J. Harrison, N. C. Handy, *Mol. Phys.* **2005**, *103*, 413.

[11] a)C. Adachi, M. A. Baldo, S. R. Forrest, M. E. Thompson, *J. Appl. Phys.* **1999**, *11*, 285; b) N. C. Greenham, R. H. Friend, D. D. C. Bradley, *Adv. Mater.* **1994**, *6*, 491.

[12] a) Y. Cao, I. D. Parker, G. Yu, C. Zhang, A. J. Heeger, *Nature* **1998**, *397*, 414; b) A. Endo, K. Sato, K. Yoshimura, T. Kai, A. Kawada, H. Miyazaki, C. Adachi, *Appl. Phys. Lett.* **2011**, *98*, 083302.

[13] a) A. S. Lukas, P. J. Bushard, E. A. Weiss, M. R. Wasielewski, *J. Am. Chem. Soc.* **2003**, *125*, 3921; b) Z. E. X. Dance, S. M. Mickley, T. M. Wilson, A. B. Ricks, A. M. Scott, M. A. Ratner, M. R. Wasielewski, *J. Phys. Chem. A* **2008**, *112*, 4194; c) S. Yin, L. Chen, P. Xuan, K. Chen, Z. Shuai, *J. Phys. Chem. B* **2004**, *108*, 9608.